

Robot Hand Fingertip Design Validation

J. Jaafar, K. Nasir and R.L.A. Shauri

Abstract Among the challenges in designing robot hand is to make it feature packed but still maintaining a compact human-hand sized without compromising its robustness. The previous work had elaborated the design process of a three-fingered robot hand until a functioning prototype is successfully produced. However, the performance of the robot hand for grasping was insufficient. This paper will discuss the enhancement in the existing design to incorporate force sensing ability with better grip-ability of the fingertip. The improved design fingertip was fabricated using rapid prototyping machine. Then, two miniature load cells were fitted into the fingertip to enable force sensing in two directions namely x -axis and z -axis. The fingertip maintains the easy-to-replace feature, improving the tip surface for better grasping and creating canal-shaped gap to have a compliant-like material effect when the fingertip is subjected to any external force. From the calibration result, it can be observed that the measured force is linearly related to the applied force in both x and z axes to prove the feasibility of the proposed design.

Keywords Miniature load cell • Sensor allocation • Easy-to-replace • Force measurement • Grasping ability

1 Introduction

Generally, robot mechanism could be divided into underactuated and fully actuated types. Dejun and Zhen [1] embarked into developing robot finger with parallelogram linkage that enable actuation from the palm. The finger has three linkages driven by one motor each to produce a total of 3-DOF. On the other hand, a

J. Jaafar · K. Nasir · R.L.A. Shauri (✉)
Faculty of Electrical Engineering, Universiti Teknologi MARA,
40450 Shah Alam, Selangor, Malaysia
e-mail: ruhizan@salam.uitm.edu.my

K. Nasir
e-mail: khairunnisanasir@yahoo.com

modified cross bar mechanism (CBM) proposed by [2] made use of parallel linkages to move the three phalanges of the robot finger. The parallel linkages applied passive prismatic joints actuated by a motor. The above underactuated finger mechanisms, however are not independent in terms of motion of each link and could hinder the built-in sensor installation when desired.

Robot hand that possesses the sense of touch is very useful for object manipulation. The installation of force sensor depends on the sensor type and the finger structure. Apart from force sensor, pressure sensor [3] and torque sensor [4] can also be used for this purpose. The Universal Robot Hand II system [5] incorporates array type tactile sensor and multi-axis force/torque sensor for force control. The design manages to cramp both sensors into the fingertip. It is a compact and practical design but the sensors used are very costly. The design of novel 2-DOF torque sensor in [6] is an interesting concept of squeezing more than one sensory ability (multi-direction detection) into one small structure. In this paper, the proposed design follows the same concept but looking into installing two miniature force sensors. The DEXMART project [7] on the other hand, make use of the commercially available optoelectronic component, LED and Photo Detectors (PD) from Honeywell to measure tendon force at the finger side. The compliant structure (flexible beam) mounted along the tendon will deform due to the tendon force measured by the LED and PD at the beam ends [8]. The selection of sensory component well suited the finger design but this design will not be practical for replaceable fingertip.

A prototype 7-DOF three-fingered robot hand has been successfully built in [9]. The mechanical design of the robot hand has been rendered feasible after going through motion tests and PID tuning. However, before furthering the work for force control, the fingertip design is modified to encase two miniature force sensors and the structure is made feasible to measure the applied force. Sensitivity, overloading and measurement error of the sensor have to be considered to avoid damage to the sensor and at the same time to get optimum output from it. Another challenge is to maintain the easy-to-replace feature of the fingertip without having to disturb the fitted sensors and avoid damage to the sensor after number of replacements. In this paper, the new fingertip design and its validation for the above will be discussed.

2 Fingertip Design

The previous design of the robot hand's fingertip has slippery surface and lack of control efficiency that causes failure in grasping. Therefore, modification of the design is required to maintain the easy-to-replace feature of the existing design, provide installation for two miniature force sensors for force control and improve the grasping capability. With acceptable maximum load of 2.2 kg, Futek LLB130 sub-miniature load cell was chosen. Two load cells were installed to measure the force in two directions namely x -axis and z -axis. The load cells were tightly fitted to

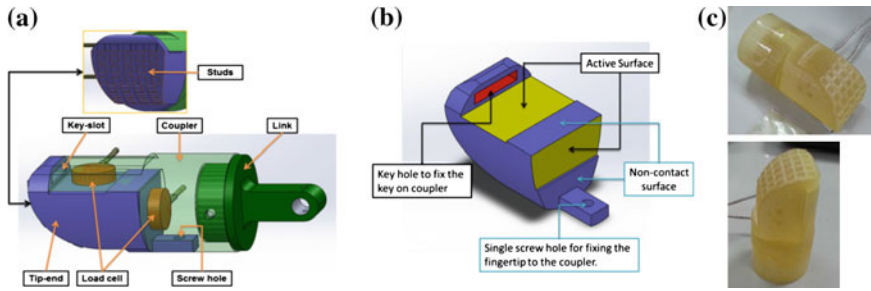


Fig. 1 New fingertip design. **a** Detailed components. **b** Active surface. **c** Actual design

the slots which were designed with the exact shape and dimension of the load cell on the fingertip; thus, it does not require any screw or rivet.

The fingertip as shown in Fig. 1a, is actually an assembly comprises of three different parts which are the link, coupler and tip-end. The link connects the whole fingertip assembly to the robot finger’s middle phalanx. The coupler attached to the link also houses the slots for load cell installation at two different locations. The final part which is the tip-end is the part with active surface and grasping studs are located. The coupler and the tip-end are fitted together using a single screw and a key-slot. Each load cell is located at two different installation slots and coupled with an active surface shown in Fig. 1b which touches the load button upon complete installation. The depth of the active surface from the non-contact surface is exactly the height of the button (0.51 mm), making sure zero output from the sensor during no-load operation. As the name designate, active surface is one of the key in the design that permits the measurement by the load cell to occur. The key-hole and the two active surfaces provide a clearance between the tip-end and the coupler when assembled. This clearance will allow the tip-end to deform when it is subjected to an external force or loading. The deformation will cause the active surfaces to displace in proportion to the magnitude of the external force or load and press the sensitive load button on the load cells. The protruded button-shape on the load cell is the active part that senses the force exerted by mean of compression. Any load to the non-loading surface will not be measured by the load cell.

3 Calibration Test

A real-time calibration experiment was conducted to analyze the response of each sensor installed in the fingertips under loading in two axes directions of *x*-axis and *z*-axis. The load is represented by standard weights ranging from 50 to 300 g. The calibration process is done without attaching the fingertip to the rest of the finger body. This arrangement is most reasonable to eliminate unwanted errors during calibration due to the weight and moving parts of the robot finger. However,

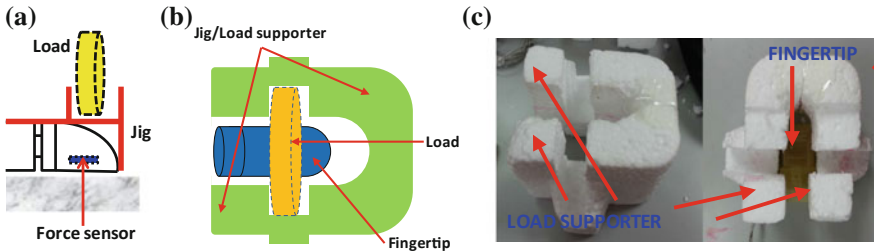
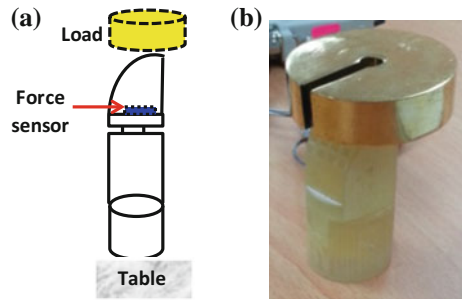


Fig. 2 Setup experiment (x-axis direction). **a** Side view. **b** Top view. **c** Actual jig (side and top views)

Fig. 3 Setup experiment (z-axis direction). **a** Illustration of loading. **b** Actual setup



without the finger body, a suitable jig is required to hold the load on the active surface consistently. Two different setups of the validation phase were conducted separately for varying amount of weights from 0 to 300 g. The calibration experiment setup for the x-axis direction is illustrated in Fig. 2. The jig is designed to hold the load in order for the force to be applied perpendicularly onto the movable slot. It should not have any contact with the fingertip that could affect the sensitive load cell measurement. Several modifications have been made on the dimensions of the jig shown in Fig. 2c. Part of the external force from the load will be distributed onto the jig due to the round shape of the load and the curvature of the fingertip surface. However, the calibration experiments have been applied where only minimum force is distributed onto the jig by avoiding contact between the fingertip-jig and jig-load. As the error introduced by the jig during loading is acknowledged, the results obtained are acceptable for validation.

Meanwhile, the calibration experiment setup for the z-axis direction is illustrated in Fig. 3. The very end of the fingertip is purposely designed to be flat to enable effective grasping of small object. Thus, the load in this experiment can steadily rest on the fingertip without the use of any jig. During the calibration tests, the force measurements were taken when force is applied normal to the load cell in both axis directions to ensure the designed active surface is compatible to the sensing behavior of the load cell. Any force applied to the fingertip not normal to or in between the sensors requires more advanced investigation in future work.

4 Result and Discussion

Figure 4a and b provide the results obtained from the real-time calibration experiments for *x*-axis and *z*-axis, respectively. Both figures depict the load used in terms of weight (grams) and the corresponding voltage (volts) sensed by the load cell versus time (*t*). The voltage drops that happened at several time intervals (such as 2–2.6 s) are due to the load that was removed temporarily for the next loading. This also causes some sharp spikes of voltages due to the very sensitive force sensor. Regardless of the disturbances, it can be shown that the movable slot could successfully return back to its initial condition when the applied load is removed from the fingertip. The experiments also proved that the installed sensor could provide the force measurement according to the applied loads ranges from 50 to 300 g. The measurement details are tabulated in Tables 1 and 2 for *x*-axis and *z*-axis, respectively.

For *x*-axis, Table 1 indicates the initial value of 0.3188 V when no load is applied due to the close fitting of the slot and the sensor. Deviation in the output voltage ranges from 0.1476 to 0.2062 V for every 50 g increments. Meanwhile, for *z*-axis, Table 2 indicates the initial value of 0.2060 V when no load is applied.

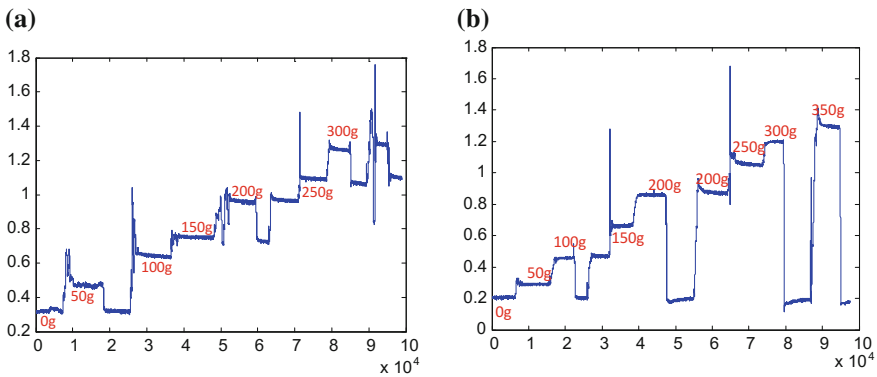


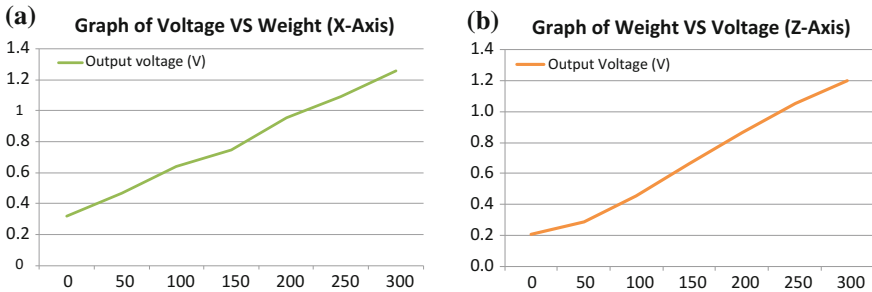
Fig. 4 Calibration results: measured voltage (V) (*vertical*) versus time (*t*) (*horizontal*). **a** *x*-direction. **b** *z*-direction

Table 1 Data collection on *x*-axis direction

| No | Weight (g) | Output (V) |
|----|------------|------------|
| 1 | 0 | 0.3188 |
| 2 | 50 | 0.4664 |
| 3 | 100 | 0.6387 |
| 4 | 150 | 0.7481 |
| 5 | 200 | 0.9543 |
| 6 | 250 | 1.0910 |
| 7 | 300 | 1.2595 |

Table 2 Data collection on z-axis direction

| No | Weight (g) | Output (V) |
|----|------------|------------|
| 1 | 0 | 0.2060 |
| 2 | 50 | 0.2913 |
| 3 | 100 | 0.4592 |
| 4 | 150 | 0.6648 |
| 5 | 200 | 0.8628 |
| 6 | 250 | 1.0514 |
| 7 | 300 | 1.2002 |

**Fig. 5** Relationship between output voltage (V) (*vertical*) and applied load (g) (*horizontal*). **a** *x*-direction. **b** *z*-direction

Deviation in the output voltage ranging from 0.0853 to 0.2056 V occurs for every 50 g increment. Both cases have non-proportional linear relationship between the voltage and applied load as graphed in Fig. 5. However, the linearity of both lines is slightly affected by the nonlinear friction of the movable slot which requires further improvements on the design and the calibration setup.

5 Conclusion

Calibration results and analysis showed that the proposed fingertip mechanical design is rendered feasible for force detection in both directions of *x*-axis and *z*-axis. In addition, the proposed design has been proven to be a successful enhancement from the existing fingertip by introducing two sensors without compromising any feature and capability. A linear relationship between applied load weight and measured voltage has been obtained. However, the fingertip design and calibration setup need to be further improved for better linearity.

Acknowledgment This research was supported by Ministry of Higher Education fund (600-RMI/FRGS 5/3 (86/2013)). The authors would also like to thank Research Management Institute (RMI) and Faculty of Electrical Engineering, Universiti Teknologi MARA for providing the financial supports and equipment to conduct this research.

References

1. Dejun M, Zhen H (2007) A new type of parallel finger mechanism. In: IEEE international conference on robotics and biomimetics, 2007. ROBIO 2007, pp 584–588
2. Bandara DSV, Gopura RARC, Kajanathan G, Brunthavan M, Abeynayake HIMM (2014) An under-actuated mechanism for a robotic finger. In: 2014 IEEE 4th annual international conference on cyber technology in automation, control, and intelligent systems (cyber), 2014, pp 407–412
3. Kobayashi D, Watanabe K, Kobayashi K, Kurihara Y (2011) Impedance force control of robot hand using pressure sensor. In: Proceedings of SICE annual conference (SICE), 2011, pp 1981–1984
4. Kanno H, Nakamoto H, Kobayashi F, Kojima F, Fukui W (2013) Slip detection using robot fingertip with 6-axis force/torque sensor. In: Robotic intelligence in informationally structured space (RiiSS), 2013 IEEE workshop, pp 1–6
5. Fukui W, Kobayashi F, Kojima F, Nakamoto H, Maeda T, Imamura N, Sasabe K, Shirasawa H (2011) Fingertip force and position control using force sensor and tactile sensor for universal robot hand II. In: IEEE workshop on robotic intelligence in informationally structured space, pp 43–48
6. Kim T-K, Kim B-S, Choi S, Kim D, Hwang J-H (2012) 2-DOF torque sensor for precise force control of robot hand. In: IEEE international conference on automation science and engineering, pp 892–895
7. Palli G, Pirozzi S, Natale C, De Maria G, Melchiorri C (2013) Mechatronic design of innovative robot hands: integration and control issues. In: IEEE/ASME international conference on advanced intelligent mechatronics, pp 1755–1760
8. Palli G, Pirozzi S (2012) A miniaturized optical force sensor for tendon-driven mechatronic systems: design and experimental evaluation. *Mechatronics* 22(8):1097–1111
9. Jaafar J, Shauri RLA (2013) Three-fingered robot hand for assembly works. In: IEEE 3rd international conference on system engineering and technology, pp 237–241